Colloids and Surfaces A: Physicochemical and Engineering Aspects 610 (2021) 125747

Contents lists available at ScienceDirect

Colloids and Surfaces A: Physicochemical and Engineering Aspects

journal homepage: www.elsevier.com/locate/colsurfa

Role of surfactant adsorption and surface properties for the efficiency of PDMS-silica antifoams

N. Politova-Brinkova [a], M. Hristova [a], V. Georgiev [a], S. Tcholakova [a,*], N. Denkov [a], M. Grandl [b], F. Achenbach [b]

[a] Department of Chemical and Pharmaceutical Engineering, Faculty of Chemistry and Pharmacy, Sofia University, 1J. Bourchier Ave., 1164, Sofia, Bulgaria
[b] Wacker Chemie AG, Johannes-Hess-Straße 24, 84489, Burghausen, Germany

HIGHLIGHTS

- Antifoam (AF) activity depends on the density of surfactant adsorption layers.
- The AF works better for surfactant adsorption layers with larger area-per-molecule.
- The mode of action of the studied PDMS-based AF is bridging-stretching.
- Spreading of PDMS-based antifoams on condensed adsorption layers is hindered.
- Fatty acids added as cosurfactants can form Ca-soaps with own antifoam activity.

GRAPHICAL ABSTRACT

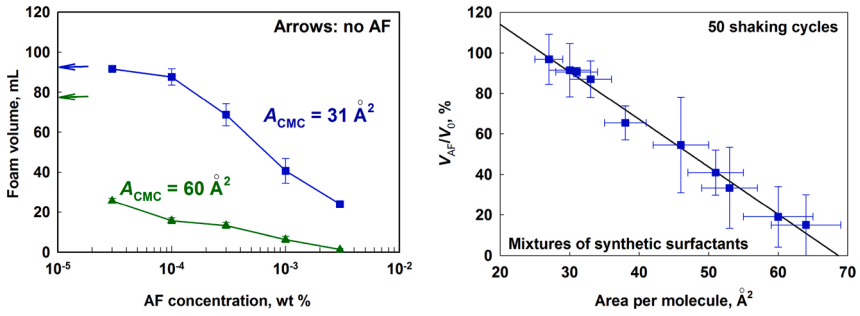

ARTICLE INFO

Keywords:
Antifoam
Surfactant adsorption
Surface modulus
Spreading
Saponin

ABSTRACT

We study how the composition of various surfactant mixtures affects the efficiency of mixed PDMS–silica antifoam in foamed surfactant solutions. First, systematic experiments are performed to characterize the surface and foam film properties of the studied surfactant solutions. The spreading, bridging and entry coefficients are calculated and the spreading ability of the antifoam is characterized by microscopy observations and by surface tension measurements. Next, the initial antifoam activity and the antifoam durability are characterized in foam tests. The obtained results reveal that the antifoam efficiency in solutions of low-molecular mass surfactants with low surface dilatational modulus depends strongly on the density (area-per-molecule) of the respective adsorption layer. The addition of nonionic surfactants, which increase the mean area-per-molecule in the mixed adsorption layer, enhances significantly the antifoam activity and durability. In contrast, the addition of surfactants, which decrease the mean area-per-molecule, suppresses the antifoam activity. Furthermore, we found that surfactant mixtures which form condensed adsorption layers on the solution surface suppress strongly the antifoam activity. As an extreme, the condensed adsorption layer formed from the natural surfactant *Quillaja* saponin suppresses the antifoam spreading even at highly positive spreading coefficient which results also in very poor AF efficiency. The obtained results rationalize in a coherent way the observed differences in the AF activity and durability in mixed solutions of various ionic, nonionic and zwitterionic surfactants.

* Corresponding author at: Department of Chemical and Pharmaceutical Engineering, Faculty of Chemistry and Pharmacy, Sofia University, 1James Bourchier Ave., 1164, Sofia, Bulgaria.
E-mail address: SC@LCPE.UNI-SOFIA.BG (S. Tcholakova).

https://doi.org/10.1016/j.colsurfa.2020.125747
Received 30 August 2020; Received in revised form 4 October 2020; Accepted 12 October 2020
Available online 18 October 2020

1. Introduction

The formation of excessive foam is a serious problem in many technological areas, e.g. in pulp and paper production, industrial painting, oil and gas production, motor lubrication, etc. [1]. Therefore, antifoam (AF) substances are deliberately used to suppress the foam formation in the respective technological processes. Antifoams are used also as essential ingredients in numerous commercial products, incl. detergents, pharmaceuticals, paints and many others [1].

Typical antifoam consists of hydrophobic oil, hydrophobic solid particles, or a mixture of both [1,2]. The mixed oil-solid particle compounds are usually much more efficient in comparison with their individual components [1–4]. The synergy of the oil and solid particles in such mixed compounds is explained with the "pinning" effect of the solid particles which lowers the entry barrier for the mixed antifoam globules, whereas the deformability and the spreading ability of the oil ensures the formation of unstable oil bridges which eventually lead to foam film rupture and foam collapse [1,3,4]. The solid particles, such as silica particles, calcium soaps, etc. act through the so-called "bridging-dewetting mechanism" [1,5–7], while the oil-based antifoams usually break the foam films via the "bridging-stretching" mechanism [8], although the "bridging-dewetting" mechanism with oil lenses is also possible [1]. The oil spreading on the surface of the foaming solution is known to enhance strongly the antifoam effect and several spreading-related mechanisms are discussed in the literature [4,9–11].

Two key physicochemical characteristics of the antifoams are (1) the so-called "entry barrier" which shows how difficult it is for pre-dispersed antifoam globules to enter the foam film surfaces and (2) the so-called "bridging coefficient" which characterises the stability of the oil bridges formed inside the foam films [1,4,12,13]. The antifoams which have low entry barrier < 20 Pa usually act as fast antifoams, whereas the antifoams with higher entry barrier act as slow antifoams [4,12–14]. The fast antifoams destroy the foam films within seconds in the early stages of the film thinning process. As a result, the foams are usually destroyed completely for less than 30 s in the presence of fast antifoams. In contrast, the slow antifoams destroy the foams only after the antifoam globules are first entrapped and compressed by the shrinking walls of the Plateau borders and nodes, in the relatively slow process of foam drainage which typically takes minutes and dozens of minutes [4, 12–14].

The entry barrier is governed by the stability of the asymmetric oil-water-air film (often called "pseudo-emulsion" film), formed between the surface of the oily globule and the foam film surface [1,12–16]. Therefore, the respective entry barrier depends on various factors which affect the stability of these asymmetric films, such as the presence of cosurfactants, electrolytes and solid particles; the size of the oily antifoam globules (the bigger in area films are less stable); and the chemical nature of the oil [1,4,10,12–14,17,18]. In our previous studies [9,10,12, 19] we quantified some of these effects and showed that various co-surfactants, such as the nonionic dodecanol and the zwitterionic cocoamidopropyl betaine (CAPB), lead to significant increase of the entry barrier for silicone oil drops, dispersed in solutions of the main anionic surfactants, sodium dodecylsulfate (SDS) or sodium dodecyl-trioxyethylene sulfate (SDP3S) [9,19]. These results were explained with the attraction between the adsorbed molecules of the anionic surfactant and the nonionic or zwitterionic cosurfactants inside the adsorption layers, formed on the bubble surfaces – this attraction leads to formation of more compact adsorption layers and to higher entry barrier [19]. Clear positive correlation was observed between the magnitude of the entry barrier of the oil drops and the foam stability [1, 4,12,19,20].

The addition of appropriately hydrophobized silica particles (typically ca. 4 wt. %) in the silicone oil decreases significantly the entry barrier of the formed antifoam globules [4,14] with resulting much higher antifoam activity in the foam tests, under otherwise equivalent conditions. Such mixtures are often termed in the literature "PDMS-silica compounds". Furthermore, in the course of foam destruction, partial segregation of the solid particles and the oil was observed, which resulted in loss of AF activity – process called in the literature "AF exhaustion" while the persistence of the antifoam to destroy newly formed foam is called "AF durability" [21]. In this process of oil-silica segregation, two populations of inactive AF globules were observed to form: (1) silica-free drops which have high entry barrier and (2) gelled silica-enriched globules which cannot break the foam films, because they are non-deformable and cannot realize the bridging-stretching mechanism which requires stretching of the oil bridges under the action of unbalanced capillary pressures [22].

The current paper builds over these previous studies by investigating systematically how the main properties of the surfactant adsorption layers affect the efficiency (activity and durability) of mixed antifoam compounds. We selected a series of surfactant solutions which exhibit different density and dilatational elasticity of their adsorption layers, formed on the air-water interface, and quantify the antifoam efficiency of typical PDMS-silica compound in these solutions. Comparing the results from the foam tests with the characteristics of the adsorption layers, we reveal several important trends which can be used as guiding rules for formulating surfactant mixtures with desired efficiency of a given PDMS-silica compound.

Note that antifoams are used in many applications to keep the foam under control, rather than to completely destroy it – obvious examples are the powders for washing machines where certain foam is needed to provide a visual clue for the washing activity of the surfactants. Therefore, the revealed trends can be used for a rational design of surfactant mixtures with desired level of foam under defined foaming conditions.

2. Materials and methods

2.1. Materials

Series of surfactant mixtures was carefully selected to provide a variation of the key surface properties of the foamed solutions in wide ranges. The individual surfactants in these mixtures include the anionic surfactants Linear Alkyl Benzene Sulfonate (LAS, technical grade, product of Aldrich), Sodium Lauryl Ether Sulfate with 1 EO group (SLES, 70 % active, product of Stepan) and Sodium Dodecyl Sulfate (SDS, product of Acros Organics); the zwitterionic surfactant Cocoamidopropyl betaine (CAPB, 40 % active, provided by In-Cosmetics OOD, Plovdiv, Bulgaria); the nonionic surfactant Isotridecyl alcohol + 8 EO groups (IT8); the natural surfactant *Quillaja* Saponin (QS, product of Desert King); and the following series of fatty acids as cosurfactants: myristic acid (MAc, C14Ac, product of Sigma-Aldrich, purity $\geq$ 95 %), palmitic acid (PAc, C16Ac, product of Riedel-de-Haën, purity $\geq$ 98 %) and stearic acid (StAc, C18Ac, product of Acros Organics).

Two sub-series of surfactant mixtures were prepared. The first series is based on the mixture of SLES + CAPB which is used in many personal care products, e.g. shampoos and body washes. These personal care formulations are typically used at a concentration of 0.5 wt. % and natural pH $\approx$ 6. The second series consists of several LAS-containing mixtures which are used in machine-washing and hand-washing applications. These washing formulations are typically used at lower surfactant concentration of ca. 0.17 wt. % and higher pH $\approx$ 8 to ensure best efficacy at minimum surfactant level. Furthermore, the performance of LAS-containing products is known to be strongly affected by the presence of Ca^{2+} ions of low concentrations. Therefore, the foamed solutions were prepared differently for the SLES + CAPB and LAS-containing mixtures, as explained below, to reflect as close as possible the solution compositions during their actual applications. Note that the used measure of the antifoam activity is weakly dependent on surfactant concentration, as explained in Section 3.3.2. Therefore, the difference in the total surfactant concentrations used in these two sub-series of solutions, 0.5 wt. % vs. 0.17 wt. %, does not affect the final conclusions of the current study.

The following concentrated stock solutions of surfactant mixtures were first prepared: 2:1 by weight of SLES + CAPB (abbreviated in the paper as SC); 2:1:0.33 SLES + CAPB + MAc (SCM); 1:1 of LAS + SLES (LS); 1:1:0.07 of LAS + SLES + MAc (LSM); 1:1:1 of LAS + SLES + CAPB (LSC); 1:1:1:0.1 of LAS + SLES + CAPB + MAc (LSCM); 1:1:2.94 of LAS + SDS + IT8 (LSI); and QS. The total surfactant concentration in all these stock solutions was 10 wt. %, except for LSI in which it was 28.3 wt. %. All these concentrates were prepared with deionized water, purified by Milli-Q Organex system (Millipore Inc., USA). In all LAS-containing formulations: LS, LSM, LSC, LSCM and LSI, the pH was set to 8.0 ± 0.2 by addition of 100 mM $NaHCO_3$, except for LSI where 34 mM citric buffer and 5.6 % 1,2-propanediol were present. The pH of the SC and SCM concentrates was not adjusted and it was 6.0 ± 0.2. The QS concentrate had natural pH ≈ 5 and it was also not adjusted before dilution for the actual surface and foaming experiments.

The concentrated LAS-containing solutions were diluted for the actual experiments down to 0.17 wt. % of total surfactant concentration using Ca^{2+} solutions of different concentrations (in most cases 0.54 mM or 0.71 mM). In the case of QS, we also used Ca^{2+} solutions for dilution down to 0.17 wt. % surfactant. In some experiments with QS, we added also100 mM $NaHCO_3$ in the diluting medium to obtain pH ≈ 7 in the final working solutions. As explained above, the SC and SCM concentrates were diluted with deionized water (in the absence of Ca^{2+}) to obtain working solutions with 0.5 wt. % total surfactant concentration and pH ≈ 6.0.

In one series of experiments, aimed to investigate the role of surfactant concentration, we varied the total surfactant concentration in the foamed solutions between 0.01 wt. % and 0.17 wt. %, while all other conditions (pH, Ca^{2+} concentration, temperature) were fixed.

The used AF compound (product of Wacker GmbH) contained linear PDMS with viscosity of 8000 mPa·s and pyrogenic hydrophobic silica particles. We dosed the AF into the foamed surfactant solutions at different AF concentrations in the range between 3×10^{-5} wt. % and 3×10^{-3} wt. %, as explained in the text. In some series of experiments, where very low AF concentrations were needed, the AF was pre-dispersed at 10 wt. % in the solvent Ethyl Methyl Ketone (EMK, Valerus, Bulgaria) to ensure more precise dosing into the foamed solution. Dedicated experiments found no effect of the EMK on the foaming behaviour at the concentrations used.

Most experiments were performed at temperature of 40 °C which is typical for many machine-washing and hand-washing protocols. Some experiments were performed at 25 °C, as explained in the text, either to check for the effect of temperature or because of technical difficulties to work at elevated temperature. For example, the interfacial tension measurements by capillary tensiometry could not be performed at high temperature, due to instability in the measured very low values of the capillary pressures.

2.2. Methods and procedures

2.2.1. Equilibrium and dynamic surface tensions of the solutions

The equilibrium surface tension (SFT), σ_{AW}, of the surfactant solutions was measured by the Wilhelmy plate method on a tensiometer K100 (Krüss GmbH, Germany). The surface tension was measured up to 900 s of surface age to reach equilibrium values. The dynamic surface tension of the surfactant solutions, $\sigma(t)$, was measured by the maximum bubble pressure method (MBPM) on a tensiometer BP2 (Krüss GmbH, Germany). These measurements were performed at both $T = 25 \pm 0.5$ °C and $T = 40 \pm 0.5$ °C.

2.2.2. Interfacial tension at the oil-water interface

In these systems we cannot apply the widely used drop-shape analysis (DSA) to measure interfacial tensions, σ_{OW}, because PDMS and water have very similar mass densities and the oil drops remain spherical in the water phase, even when these drops are of millimetre size. Therefore, the Capillary Pressure Tensiometry (CPT) was used which includes formation of a spherical drop of PDMS in the aqueous surfactant solution and measuring its capillary pressure by a pressure transducer [23–26]. We used the CPT module of the instrument DSA100R (Krüss GmbH, Germany). These measurements were performed at $T = 25 \pm 0.2$ °C only, because CPT method gave scattered results when tried at 40 °C, due to the high sensitivity of the pressure measurements at O/W interface to small temperature fluctuations.

2.2.3. Surface dilatational modulus of the solutions

The surface dilatational moduli of the surfactant solutions were measured by the oscillating drop method on DSA10 instrument, equipped with ODM/EDM module (Krüss GmbH, Germany) [25–27]. From this experiment we obtain values for the surface elastic modulus (G', related to surface elasticity) and surface viscous modulus (G'', related to surface dilatational viscosity, $\mu_{SD} = G''/\omega$) of the surfcodulus is defined as:

$$G = \left[(G')^2 + (G'')^2\right]^{1/2} \quad (1)$$

The relative surface area amplitude was varied in the range of 2–10 % and the period of deformation was fixed at 5 s. The temperature during the measurements was kept constant, $T = 40 \pm 0.2$ °C or 25 ± 0.2 °C, via a thermostating chamber TA10 (Krüss GmbH, Germany).

2.2.4. Observation of foam films in capillary cell

Foam films were formed and observed in the capillary cell of Scheludko-Exerowa [28]. The inner radius of the capillary which acts as a film holder was R =1.5 mm and the typical radius of the foam films formed in this capillary was $R_F \approx 0.15$ mm. The foam films were observed in reflected light with optical microscope Axioplan (Zeiss, Germany), equipped with a long-distance objective Zeiss Epiplan 20×/0.40, CCD camera (Sony SSC-C370 P) and H-264 Digital Video Recorder. By analysing the intensity of the reflected light, we determined the foam film thickness [28]. The behaviour and the stability of the foam films were studied both in the presence and in the absence of pre-dispersed AF entities in the surfactant solutions.

These experiments were performed in two configurations – with closed and with open to the atmosphere capillary cell. In a closed cell, the capillary pressure (the one that sets the equilibrium film thickness) is around 50 Pa for foam films. As shown in ref. [29], in an open cell the compressing capillary pressure could increase up to 50 000 Pa, due to the water evaporation from the foam film. All these experiments were performed at room temperature ≈ 25 ± 1 °C.

2.2.5. Determination of the spreading ability of the AF

2.2.5.1. Via surface tension measurements. We used the Wilhelmy plate method to characterize the spreading dynamics of the AF on the solution surface. In these experiments, we measured the surface tension of a given surfactant solution (first, without AF added) for 200 s at 40 ± 1 °C or 25 ± 1 °C. Afterwards, we deposited small amount of the studied AF on the solution surface using a needle. The subsequent evolution of the surface tension was monitored for at least 500 additional seconds.

2.2.5.2. Via microscope observations. We observed the process of antifoam spreading on the solution surface using optical microscope Axioplan (Zeiss, Germany), equipped with a long-distance objective Zeiss Epiplan 20×/0.40, CCD camera (Sony SSC-C370 P) and H-264 Digital Video Recorder. The surfactant solution was poured in a Petri dish and, afterwards, small amount of AF was deposited on the surface using a needle. The spreading of the oil on the solution surface was observed in reflected light for about 5 min at magnification ×20. These experiments were conducted at ambient temperature (25 ± 1 °C).

2.2.6. Foaming experiments

2.2.6.1. Preparation of the foaming solution. To characterize the

foamability of the surfactant solutions without AF, we diluted the concentrated surfactant solutions down to the working concentration with deionized water or with Ca^{2+} solution, as explained in Section 2.1. The standard working surfactant concentration was 0.5 wt. % for the SLES + CAPB solutions (SC and SCM) or 0.17 wt. % for all LAS-containing and QS solutions. In the experiments aimed to clarify the effect of total surfactant concentration, the latter was varied between 0.01 wt. % and 0.17 wt. %, at fixed ratio of the surfactant components.

In the foaming experiments with added AF, we pre-dispersed the antifoam in the concentrated surfactant solutions and applied over-night mild stirring on a magnetic stirrer. The AF was dosed in the surfactant concentrate using a micropipette (Eppendorf® Multipette® M4). For the actual foaming experiments, these concentrates were diluted down to the working concentration. In the experiments in which the AF concentration was rather low, we pre-dispersed 10 wt. % of the AF compound in EMK solvent (EMK) before dosing the AF into the surfactant concentrate – thus, we ensured more precise dosing and better reproducibility of the results from the foam tests, aiming to evaluate the AF activity and durability. Depending on the specific aim of the experiment, we either worked at fixed AF concentration of 3×10^{-4} wt. % or varied it in the range between 3×10^{-5} wt. % and 3×10^{-3} wt. %.

2.2.6.2. Foam tests and determination of the AF activity and durability. We used automated Bartsch test [30] to evaluate the foaming ability of the surfactant solutions and the effect of the antifoam. Custom-made automatic device shakes 130 mL glass cylinder, mounted on a holder. This holder is moved by a motor, so that the cylinder axis changes its angle with respect to the vertical in a cyclic way: from 0° in the initial vertical position of the cylinder, through 90° (horizontal cylinder), up to 135° (bottom higher) and back. Because the inclination of the cylinder axis continuously changes during the cycle, the solution moves and splashes inside the cylinder. The foam is produced mostly at the moments when the solution hits the top and the bottom of the cylinder, at the end of each semi-cycle [30]. The frequency of the cylinder cyclic motion and the number of cycles are pre-defined using the control panel of the instrument. In these experiments, the volume of the surfactant solution inside the cylinder was 10 mL and the shaking period was fixed at 1.23 s (frequency of 0.813 s^{-1}).

The foamability of the studied systems was characterized by the volume of air trapped in the solution, calculated by subtracting the volume of the solution (10 mL) from the total measured volume (solution + foam). Most of the experiments were performed at starting temperature of 40 °C which gradually decreased during the experiment.

For given surfactant solution we performed up to 50 shaking cycles in the absence of AF, because this number of cycles was sufficient to reach maximum volume of the foam formed, and up to 1000 shaking cycles in the presence of AF when the foam volume slowly increased, due to the gradual exhaustion of the AF. To quantify the initial AF activity in a given surfactant solution, we compared the foam volumes with and without AF, after 10 and 50 shaking cycles. The AF durability was characterized as explained in Section 3.3.3 below.

3. Results and discussion

3.1. Surface properties of the surfactant solutions

3.1.1. Surface tension isotherms

The surface tension isotherms were measured at 40 °C using the Wilhelmy plate method. To determine the equilibrium surface tension at given surfactant concentration, we assumed diffusion limited adsorption and extrapolated to infinite times the experimental data for the surface tension, as a function of the reciprocal square root of time, $1/\sqrt{t}$ [31]. The equilibrium surface tension isotherms, determined by this procedure, are shown in Fig. 1.

The surface adsorption and the average area-per-molecule in the equilibrium adsorption layers were determined using the simplest version of the Gibbs adsorption isotherm to fit the steepest region in the experimental isotherms, see Fig. 1:

$$\frac{d\sigma_{AW}}{d\ \ln C} = -k_B T\ \Gamma \tag{2}$$

Here σ_{AW} is the equilibrium surface tension, C is the total surfactant concentration, k_B is the Boltzmann constant, T is the temperature, and Γ is the total surfactant adsorption. Eq. (2) is strictly valid for mixtures of nonionic surfactants [30].

Usually, Eq. (2) requires modifications when ionic surfactants are involved. However, it turned out that for our systems we could use Eq. (2) with reasonable accuracy even for the surfactant mixtures containing ionic surfactants. The reason is that the Ca^{2+} ions present in the LAS-containing solutions are known to displace the sodium ions (introduced with the surfactant) from the surfactant adsorption layers [32, 33]. A very illuminating illustration of this effect of Ca^{2+} ions is Fig. 3 in [32] which shows that the LAS adsorption isotherms do not change while varying the concentration of NaCl as a background electrolyte. As a result of this complete displacement of the Na^+ ions from the adsorption layers, the ionic surfactants in these solutions co-adsorb with Ca^{2+} counterions which have fixed concentration and, hence, (almost) fixed chemical potential, while varying the surfactant concentration. Therefore, the change in the surface tension upon variation of the surfactant concentration in Ca-containing solutions is due only to the adsorption of the surfactant molecules, while the co-adsorbing Ca^{2+} ions do not contribute, because the term $\Gamma_{Ca} d\mu_{Ca} \approx 0$, due to the fixed concentration of the Ca^{2+} ions.

For the CAPB-containing solutions (SC and SCM), which do not contain Ca^{2+}, the arguments are different but lead to a similar conclusion. The formation of mixed SDS + CAPB adsorption layers in the presence of Na^+ counterions is studied in detail by Danov et al. [34]. These authors showed that at concentrations approaching the critical micellization concentrations (CMC) of the surfactant mixtures, the adsorption layers contain around and above 90 % of the zwitterionic CAPB molecules, whereas the relative fraction of the anionic surfactant in the adsorption layer is around 10 % or lower. Accordingly, the occupancy of the Stern adsorption layer by Na^+ ions is very low, typically 5–10 %. Thus, we see that such mixed adsorption layers are dominated by the electroneutral zwitterionic surfactants, with very small contribution in the total adsorption (5–10 %) by the co-adsorbing Na^+ ions. The addition of fatty acids in these systems would not change this feature, because these fatty acids are protonated (nonionic) at the working pH ≈ 6.0 in the studied solutions.

Table 1 summarizes the obtained parameters for the equilibrium adsorption layers in the studied surfactant formulations. No significant effect of the increase of Ca^{2+} concentration from 0.54 to 0.71 mM is seen for most of the systems studied. The myristic acid in the LAS-containing mixtures, LSM and LSCM, does not change significantly any of the adsorption parameters, which is due to the relatively low fraction of myristic acid in these surfactant mixtures (around 3 %), the relatively high pH of 8.0 at which the myristic acid is partially ionized and cannot pack well within the adsorption layer of ionic surfactants as shown in our previous study [35], and due to the presence of Ca^{2+} ions which form soap precipitates with the myristic ions in the bulk and thus reduce their adsorption. Note that the SLES + CAPB mixture which contains myristic acid (SCM) has higher fraction of myristic acid (10 %), the pH ≈ 6.0 is lower, and no Ca^{2+} is added to the foamed solutions. Under these conditions, no precipitates are formed in the solution and the myristic acid acts as a cosurfactant which decreases the equilibrium surface tension, critical micellar concentration (CMC) and area-per-molecule in the adsorption layer. Furthermore, the myristic acid in these systems causes condensation of the adsorption layer and leads to high surface visco-elasticity, as found in [36] and confirmed in sub-section 3.1.2 below.

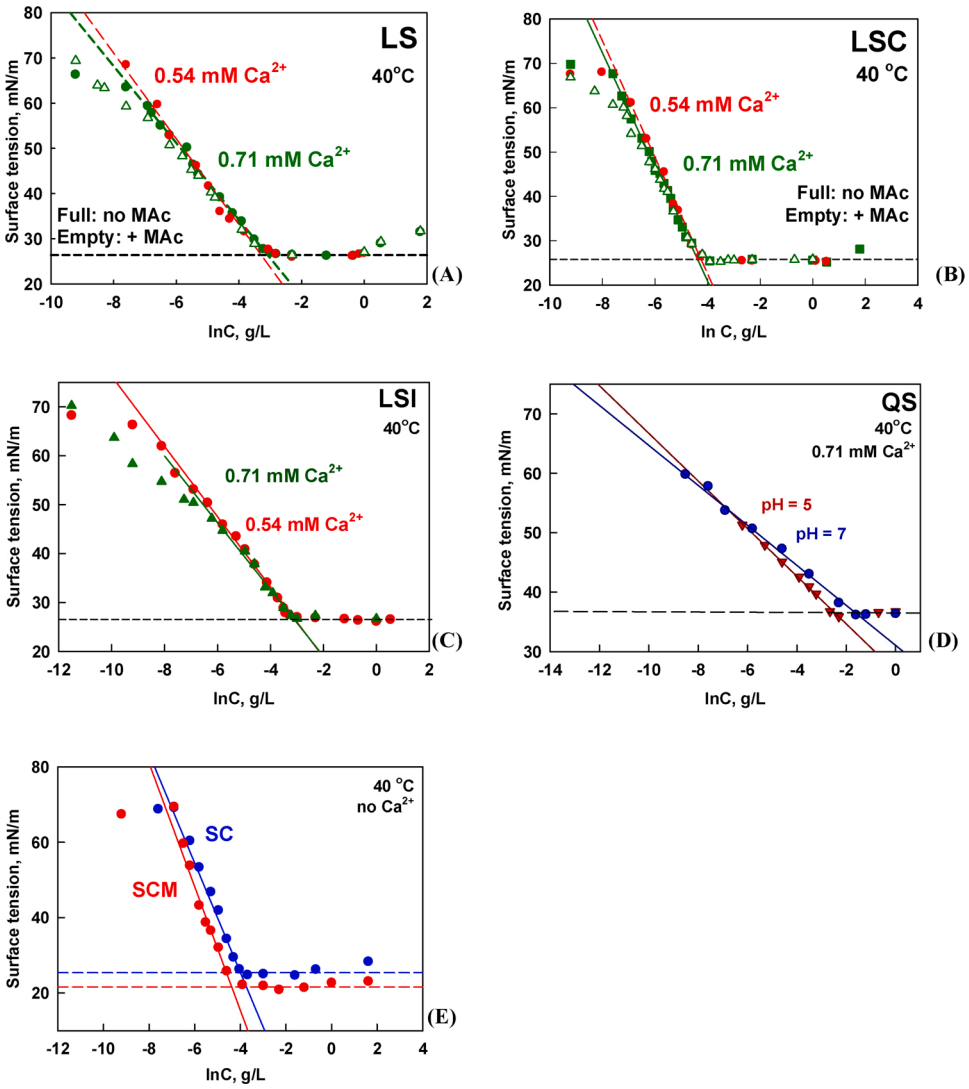

Fig. 1. Surface tension isotherms of (A) LSM, (B) LSCM, (C) LSI, (D) QS and (E) SCM mixtures. These data are measured at 40 °C in the absence of Ca^{2+} and at pH ≈ 6 for SC and SCM solutions, or in the presence of 0.54 mM or 0.71 mM Ca^{2+} at pH ≈ 8 for the other solutions, as indicated in the graphs. Results at pH ≈ 5 and pH ≈ 7 are presented for the QS system.

Table 1
Critical micellization concentration, CMC; surface tension at CMC, σ_{CMC}; average area per molecule at CMC, A_{CMC}, as determined from the surface tension isotherms using Eq. (2); and total surface dilatational modulus, G; all measured at 40 °C in the presence of 0.54 mM or 0.71 mM Ca^{2+} in the LAS-containing solutions, while no Ca^{2+} is added in the SC and SCM formulations.

System	pH	Ca^{2+}, mM	CMC, mg/L	σ_{CMC},mN/m	A_{CMC}, Å^2	Properties of the adsorption layers			
						G, mN/m	Universal surface age, t_u =10 ms		
							σ,mN/m	Γ, μmol/m^2	E_G, mN/m
LS	8.0 ± 0.5	0.54	35 ± 5	26.4 ± 0.2	46 ± 4	2.0 ± 0.2	31.4 ± 0.6	3.5 ± 0.0	159.9 ± 4.5
		0.71	47 ± 5	26.4 ± 0.2	51 ± 4	2.2 ± 0.2	31.4 ± 0.0	3.2 ± 0.0	176.8 ± 0.2
LSM		0.71	40 ± 5	26.4 ± 0.2	53 ± 4	2.2 ± 0.2	31.8 ± 0.1	3.1 ± 0.0	180.2 ± 0.8
LSC		0.54	13 ± 2	25.8 ± 0.2	31 ± 3	1.0 ± 0.2	30.0 ± 1.3	5.2 ± 0.1	116.4 ± 6.2
		0.71	13 ± 2	25.8 ± 0.2	33 ± 3	1.0 ± 0.2	29.0 ± 0.1	4.9 ± 0.0	128.7 ± 0.4
LSCM		0.71	15 ± 2	25.8 ± 0.2	38 ± 3	1.7 ± 0.2	28.8 ± 0.3	4.3 ± 0.0	149.5 ± 1.6
LSI		0.54	43 ± 3	27.0 ± 0.2	60 ± 5	1.3 ± 0.2	28.7 ± 0.4	2.8 ± 0.1	234.2 ± 3.8
		0.71	43 ± 3	27.0 ± 0.2	64 ± 5	1.3 ± 0.2	27.6 ± 0.1	2.6 ± 0.0	262.0 ± 0.9
SC	6.0 ± 0.0	0.0	18 ± 2	25.4 ± 0.2	30 ± 3	4.4 ± 0.4	33.6 ± 0.1	5.2 ± 0.1	96.5 ± 0.6
SCM		0.0	13 ± 2	22.0 ± 0.5	27 ± 2	88.4 ± 5.2	29.0 ± 0.2	5.8 ± 0.0	108.5 ± 1.1
QS	5.0 ± 0.1	0.71	100 ± 20	35.9 ± 0.5	130 ± 10	110 ± 10	62.8 ± 2.0	0.9 ± 0.1	20.1 ± 9.5
	7.3 ± 0.4	0.71	210 ± 20	36.2 ± 0.5	110 ± 10	130 ± 10	61.1 ± 1.2	1.2 ± 0.1	24.8 ± 6.0

The presence of the zwitterionic surfactant CAPB in the LSC and LSCM formulations leads to significant change in the adsorption parameters, as it decreases strongly both the CMC and the area-per-molecule when compared to the LS and LSM systems. Thus, we obtained area per molecule of ≈ 0.3 nm^2 for SC and LSC, compared to ≈ 0.5 nm^2 for LS solutions. These results indicate clearly that the zwitterionic CAPB leads to formation of much denser (but not condensed) adsorption layer, compared to the LS or LSM systems. The presence of both CAPB and nonionized myristic acid in the SCM formulation provides both high adsorption density and high surface modulus of the respective adsorption layer.

In contrast, the presence of the nonionic surfactant IT8 with voluminous head-group of 8 ethoxy-units in the LSI formulation leads to bigger area-per-molecule of ≈ 0.6 nm^2, when compared to the other mixtures of synthetic surfactants. Thus, we were able to vary the mean area-per-molecule in the mixed adsorption layers of synthetic surfactants from ≈ 0.3 nm^2 to ≈ 0.6 nm^2.

The largest area-per-molecule ≈ 1 nm^2 was determined for the QS system, see Table 1. This result, however, is not related to the formation of loose adsorption layer, but to the much bigger size and the specific lay-on orientation of the aglycon of the QS molecules, as clarified in [37].

The observed differences in the structure of the adsorption layers of the studied solutions are schematically illustrated in Fig. 2.

3.1.2. *Surface dilatational modulus of the adsorption layers*

As one can see from Table 1, the total surfactant concentration of 0.17 wt. % for the LAS-containing mixtures and 0.5 wt. % for SLES + CAPB mixtures, used in the foaming experiments, are between 1 and 3 orders of magnitude higher than the CMC of the respective surfactant solutions. For these foaming solutions we measured the surface dilatational moduli and the obtained results are shown in Table 1 and in

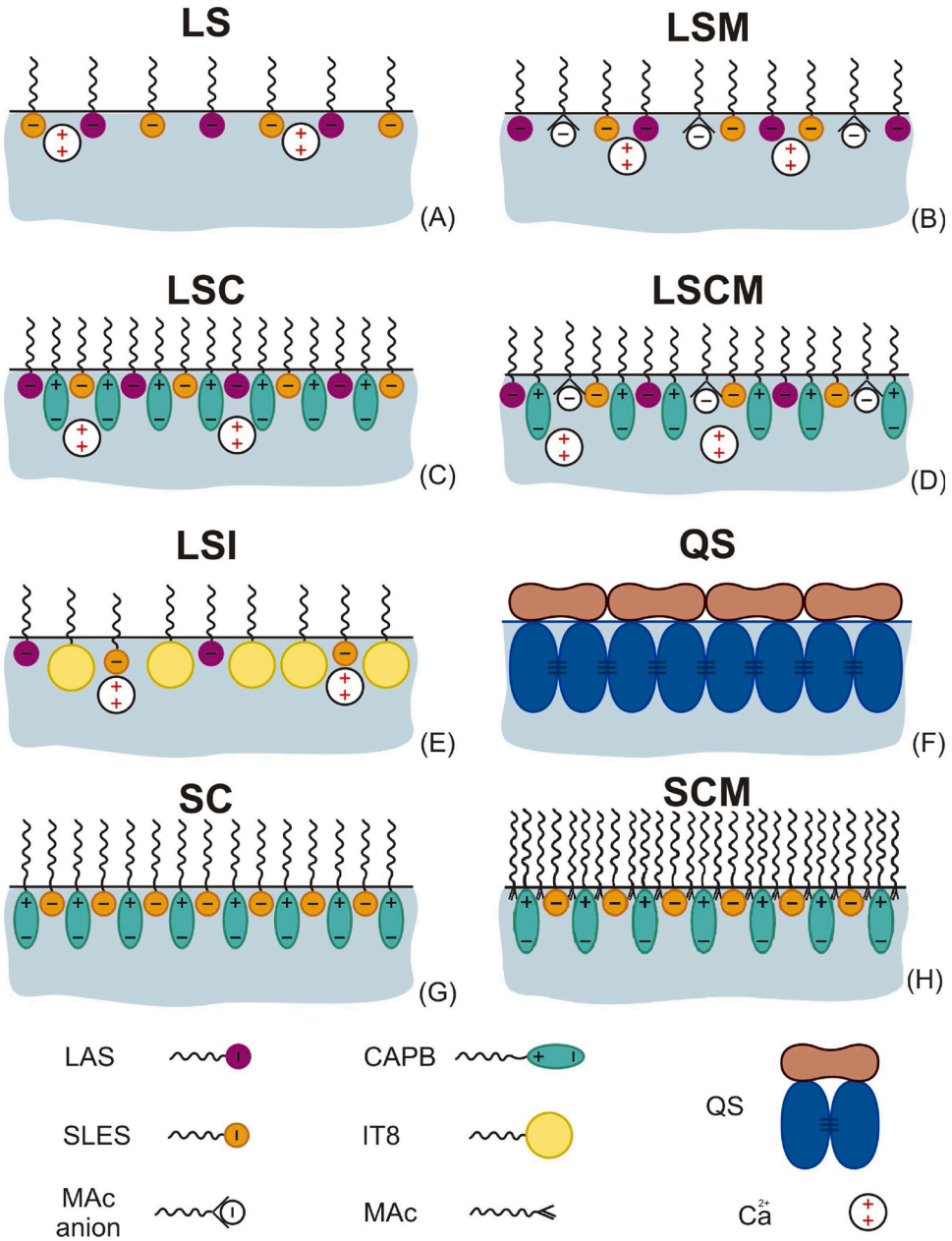

Fig. 2. Schematic presentation of the structure of the surface adsorption layers, formed on the air-water interface: (A) LS, (B) LSM, (C) LSC, (D) LSCM, (E) LSI, (F) QS, (G) SC and (H) SCM solutions. The higher surfactant density in the adsorption layer shown in (H) reflects the surface phase transition leading to condensed adsorption layer, as evidenced by the high surface modulus of the SCM surfactant system [35,36].

Fig. S1 in the Supporting Information.

For all LAS-containing mixtures with pH ≈ 8 and T = 40 °C, we measured relatively low surface dilatational moduli of several mN/m, which is due to the very fast adsorption-desorption process of the main surfactants. These results show that there is no significant attraction between the surfactant molecules within the adsorption layer and that no condensed adsorption layer is formed in the LAS-containing systems. Under these conditions, the myristic acid is ionized and is unable to promote the formation of condensed surface layer.

In contrast, much higher surface modulus, G > 100 mN/m, indicating the formation of condensed adsorption layer, was measured when adding MAc to the SC solution at pH ≈ 6 and 25 °C [35]. The adsorption layer in the SCM system is highly viscoelastic, with the surface loss modulus being higher than the surface elastic modulus (see Fig. S1 in the Supporting Information). To clarify the effect of temperature in these systems, we performed experiments at 40 °C and 20 °C and at natural pH ≈ 6 without Ca^{2+}, see Fig. S4 in the Supporting Information. For SC we measured low surface moduli, as expected, in the range of 5.5 ± 0.1 mN/m at 20 °C and 4.4 ± 0.4 mN/m at 40 °C (both measured at ≈ 1 % surface deformation). For the SCM system at 20 °C we obtained surface modulus of 237 ± 11 mN/m (at 2 % deformation) which indicates the formation of condensed mixed adsorption layer on the water-air interface. The increase of the temperature up to 40 °C leads to significant decrease of the surface modulus of the SCM solution down to 88 ± 5 mN/m, due to disturbed packing of the surfactant molecules in the adsorption layer. Such value, however, is still much higher than that of the basic surfactant formulations, LS and SC, used in the current study.

To check whether longer-chain fatty acids could increase the surface modulus and induce surface phase transition at higher pH and temperature (T = 40 °C and pH ≈ 8), we added palmitic acid (PAc), stearic acid (StAc) or mixture of these both acids to the LSC mixture and measured the respective surface moduli. Again, very low moduli of the respective adsorption layers (see Fig. S2 in the Supporting Information) were measured which means that even fatty acids with longer chain-length are unable to increase the dilatational surface moduli at pH ≈ 8 and T = 40 °C.

Summarizing, a transition between fluid and condensed adsorption layers could be induced by adding myristic acid to SLES + CAPB solution at pH 6. The increase of the temperature up to 40 °C reduces the surface viscoelasticity of the adsorption layer, while still maintaining a relatively high value.

QS solutions also show very high surface modulus, G > 100 mN/m, even at 40 °C. However, the elastic component is predominant for QS – the surface elastic modulus is more than 5 times higher than the surface loss modulus, see Fig. S1 in the Supporting Information. Measurements of the surface moduli of QS solutions with different pH values and electrolyte levels showed that these factors do not affect significantly the surface rheological behaviour in the studied range of conditions, see Fig. S3 in the Supporting Information.

3.1.3. Surface properties of dynamic adsorption layers

In a recent study [30] we showed that the foamability of surfactant solutions depends strongly on the rate of adsorption of the surfactant molecules on the air-water interface. On this basis, we proposed a new theoretical approach to quantify this effect. Very good correlation between the foamability and the transient surface coverage or the Gibbs elasticity of the dynamic adsorption layers was found in [30].

Therefore, we measured the dynamic surface tension (DST) of the studied solutions, see Fig. 3, and determined the main characteristics of the dynamic adsorption layers, formed on the bubble surfaces, using the approach from Ref. [30]. As in the previous study, we used 10 ms surface age (see Table 1) as a characteristic time for the creation of new bubble surface in the used foaming test.

The DST results showed significant difference in the kinetics of adsorption for the mixtures of synthetic surfactants, on one side, and the natural surfactant QS, on the other side. For the latter we determined much higher DST > 60 mN/m, even at t_u =10 ms, compared to ≈ 30 mN/m for the mixtures of synthetic surfactants, see Table 1 and Fig. 3. The main reason for this difference is the much bigger size and mass of the saponin molecules, compared to those of the synthetic surfactants. For the saponin system we determined relatively low adsorption of ≈ 1 μmol/m^2 and low dynamic Gibbs elasticity of ≈ 20−25 mN/m at t_u =10 ms, which is by 4–10 times lower than those of the other surfactant solutions studied, see Table 1. Among the synthetic surfactant mixtures, highest dynamic Gibbs elasticity was determined for LSI, see Table 1, which was observed to have faster adsorption compared to the other formulations, see Fig. 3. On the other hand, LSI is the system for which the loosest equilibrium adsorption layer was observed, due to the presence of the nonionic component with large head-group in this mixture.

Again, the presence of MAc in the LSM and LSCM solutions does not lead to any significant change in the DST curves under these conditions, T = 40 °C and pH ≈ 8. In contrast, the presence of MAc in the SCM mixture reduces the DST when compared to SC solution, due to the lower pH ≈ 6 and the absence of Ca^{2+} in the respective solutions.

3.1.4. Thin liquid films

To obtain information about the behaviour of the foam films, formed between two colliding bubbles, we observed the foam films in capillary cell. The foam films in the systems with low dilatational surface moduli drained to their equilibrium thickness very rapidly, within 60−80 s, and remained stable for > 600 s in closed capillary cell and for > 300 s in open cell. These foam films are electrostatically stabilized with equilibrium thickness of around 30 nm at P_C =50 Pa. For the natural surfactant QS saponin, however, we observed a different behaviour – its foam films thin down very slowly, for many minutes, and dimple (thicker central region) is observed even after the cell opening to the atmosphere. This slower drainage for QS saponins is due to the very high surface elastic modulus of its adsorption layers.

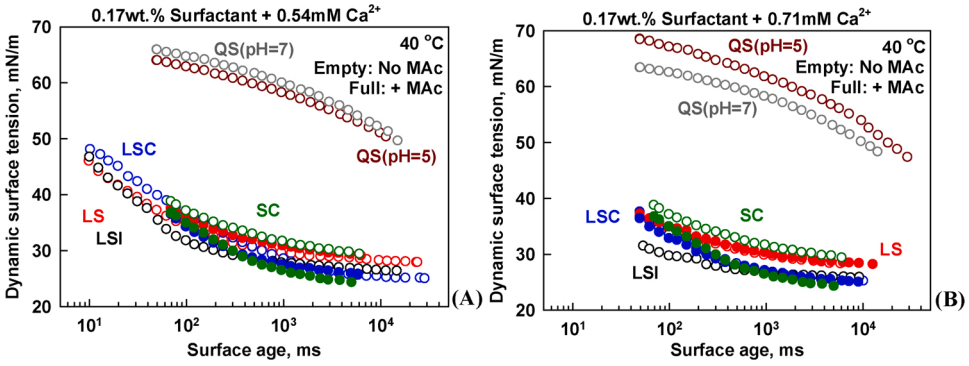

Fig. 3. Dynamic surface tension as a function of surface age for surfactant solutions prepared with (A) 0.54 mM Ca^{2+} and (B) 0.71 mM Ca^{2+} (no Ca^{2+} in the SC and SCM solutions). These data are measured at 40 °C by the MBPM.

Fig. 4 presents illustrative images of the foam films of different surfactant solutions, 60 s after their formation, and the measured drainage time to the film equilibrium thickness. One sees that the higher surface moduli of the saponin adsorption layer result in more than one order of magnitude longer drainage time of the foam films (note the logarithmic scale of the graph in Fig. 4E).

During the observations of the MAc containing systems, some crystals were observed in the solutions containing Ca^{2+} ions, due to the formation of precipitated calcium soaps. Such soap crystals could have some antifoam effect, as clarified by Miller, Garrett and co-workers [38–40].

3.2. Oil spreading and determination of the Spreading, Entry and Bridging coefficients

3.2.1. Surfactant adsorption layers on the oil-water interface

To study the surfactant adsorption layers formed on the oil-water interface, we measured the interfacial tension at the interface with the PDMS oil used to prepare the AF compound, at different concentrations of the LSI and LS mixtures in the aqueous phase. We determined the interfacial tension isotherms shown in Fig. 5. For comparison, the corresponding surface tension isotherms for the air-water interface are also presented. From these isotherms we determined the CMC, the interfacial tension at CMC, and the average area-per-molecule in the adsorption layer at the CMC using Gibbs equation, Eq. (2). In both LS and LSI systems, the CMC values determined from the interfacial tension isotherms at oil-water interface were found to be somewhat higher than the corresponding ones obtained from the surface tension isotherms (air-water interface). The latter difference is most probably due to partial solubility in the oily phase of some admixtures, present in the surfactants. For the LSI mixture we obtained significantly larger mean surface area-per-molecule for the oil-water interface, compared to the air-water one.

3.2.2. Spreading ability of the AF

We characterized the affinity of the studied AF to spread on the surface of the various surfactant solutions which is governed by the balance of the respective A/W, O/W and O/A interfacial tensions. Fig. 6A presents the results from the surface tension measurements of the synthetic surfactant solutions with low surface modulus (0.17 wt. % LS, LSM, LSC, LSCM and LSI, and 0.5 wt. % SC). One sees from Fig. 6A that the surface tension sharply decreases upon deposition of AF on the solution surface, thus indicating the instant oil spreading on the solution surface. The spreading on the SC system was slightly slower and the decrease of the surface tension was smaller when compared to the other surfactant mixtures in this series.

Very different spreading behaviour was observed with the solutions having high surface modulus: QS and SCM (see Fig. 6B). Delay in the AF spreading on the QS surface is seen and practically no spreading was observed on the SCM surface. These results are discussed below, after presenting the values of the spreading coefficients.

The optical observations of the spreading process agree with the results from the surface tension measurements. For the surfactants exhibiting distinct jump in the surface tension upon AF deposition, we

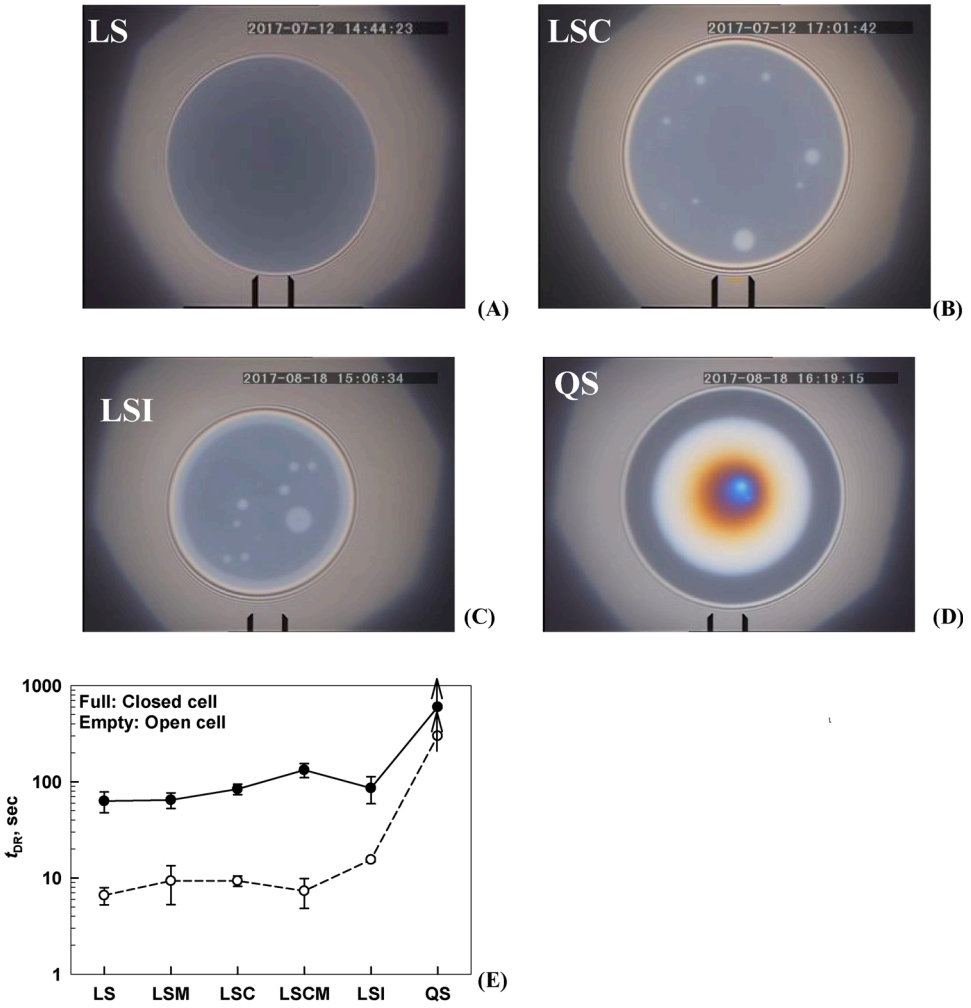

Fig. 4. Foam films as observed 60 s after their formation from (A) LS, (B) LSC, (C) LSI, and (D) QS solutions. (E) Drainage time of the foam films to their equilibrium thickness, t_{DR}, for the various surfactant systems, measured in closed and in open capillary cell. The experiments are performed at room temperature to avoid the water evaporation from the foam films. The lines connecting the symbols in (E) are drawn only to visualize the trends observed when adding cosurfactants to the main surfactant system LS = LAS + SLES.

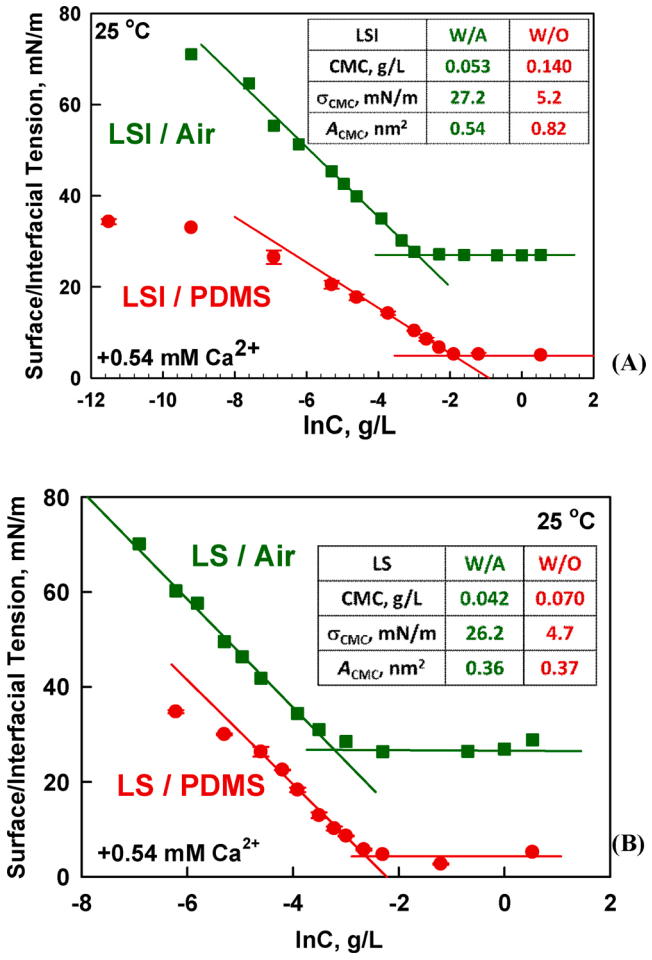

Fig. 5. Comparison of the surface and interfacial tension isotherms at W/A and W/O interfaces, respectively, for: (A) LSI and (B) LS surfactant mixtures, as measured at 25 °C.

observed the formation of continuous AF layer on the solution surface. For the SCM system, for which no change in the surface tension was detected, we observed sharp boundary between the AF lens, deposited on the solution surface, and the neighbouring solution surface which was clean of spread AF, see Fig. 6B. Similar sharp boundary was observed with the solutions of QS saponin as well. From these experiments we conclude that the studied AF spreads well on the surface of solutions with low surface dilatational moduli, while the spreading is either suppressed or it is very slow on the surface of solutions with high surface dilatational modulus (QS and SCM).

3.2.3. Determination of the entry, spreading and bridging coefficients

Spreading, entry and bridging coefficients are defined by the expressions [1,14,41–45]:

$$\text{Entry coefficient } E = \sigma_{AW} + \sigma_{OW} - \sigma_{OA} \quad (3)$$

$$\text{Spreading coefficient } S = \sigma_{AW} - \sigma_{OW} - \sigma_{OA} \quad (4)$$

$$\text{Bridging coefficient } B \equiv \sigma_{AW}^2 + \sigma_{OW}^2 - \sigma_{OA}^2 \quad (5)$$

To calculate their values for the studied AF in the various surfactant solutions, we need the interfacial tensions of all three interfaces – A/W, O/W and O/A. We measured the oil-air interfacial tension to be 20.6 ± 0.1 mN/m which agrees with the values reported in literature [46]. This tension is too low to be affected by the presence of hydrocarbon surfactants, like those used in the current study – they do not adsorb on the respective oil-air interface.

The W/O interfacial tensions at the working surfactant concentration of 0.17 wt. % in the case of LS, LSM and LSI were all measured to be in the range between 5 and 6 mN/m, while for the LSC-PDMS and LSCM-PDMS interfaces we measured lower interfacial tensions of 2.4 ± 0.3 and 1.6 ± 0.1 mN/m, respectively. Therefore, the presence of CAPB in the surfactant mixtures decreases strongly the interfacial tension. For the QS solution we measured higher interfacial tension of 10.2 ± 0.3 mN/m. The surface tension of this solution, 37.3 ± 0.2 mN/m, is also higher than that of the other solutions studied.

The calculated values of the E, S and B coefficients are compared in Table 2. All calculated entry coefficients are positive, $E > 0$, which means that the formation of oil lenses on the solution surface and the formation of oil bridges between the foam film surfaces are thermodynamically possible processes. All bridging coefficients are also positive, $B > 0$, which means that, if oil bridges are formed in the foam films, both the bridges and the foam films would be unstable.

The spreading coefficients for most of the studied systems are also positive which reflects the ability of the studied PDMS-based AF to spread on the solution surface. The only negative value of S is calculated for the SCM solution, which agrees well with the results from the actual spreading experiments, cf. Fig. 6B.

Interestingly, we measured highly positive spreading coefficient in the QS solution, $S = 6.5 \pm 0.8$ mN/m, whereas a tiny instantaneous decrease in the surface tension, followed by very slow spreading were detected with this system, cf. Fig. 6B. This suppressed spreading is probably due to the specific property of the QS adsorption layer to form highly elastic, well packed adsorption layer. Most probably, the silicone oil cannot spread directly over this adsorption layer and, at the same time, the oil is unable to displace rapidly the saponin molecules from the solution surface – the saponin adsorption layer behaves as two-dimensional elastic solid layer. To the best of our knowledge, no such resistance to spreading has been reported so far in systems with positive spreading coefficient.

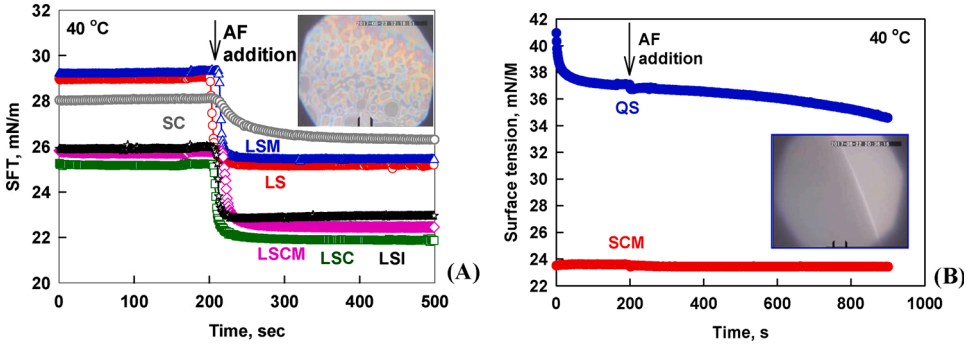

Fig. 6. Surface tension vs. time for surfactant mixtures with (A) low and (B) high surface moduli. Small drop of the AF was deposited on the solutions surface using a needle at $t = 200$ s. Data are presented for 0.17 wt. % LS, LSM, LSC, LSCM and QS, or for 0.5 wt.% SC and SCM surfactant solutions. These experiments are performed at 40 °C, pH = 8.0 and 0.71 mM Ca^{2+}, except for SC and SCM where pH = 6.0 and no Ca^{2+} was present.

Table 2
Measured interfacial tensions (IFT) and calculated Entry (E), Spreading (S) and Bridging (B) coefficients for the PDMS oil used to prepare the studied AF and 0.17 wt. % surfactant solutions in the presence of 0.54 mM Ca^{2+} (0.5 wt. % and no Ca^{2+} for SC and SCM solutions). The interfacial tensions are measured at 25 °C.

Oily phase	Water phase	IFT, mN/m (at 25 °C)				Entry coefficient, E, mN/m	Spreading coefficient, S, mN/m	Bridging coefficient, B, mN^2/m^2
		Oil / pure water	O/W	W/A	O/A			
PDMS	LS	37.2 ± 0.3	5.2 ± 0.1	29.6 ± 0.2	20.6 ± 0.1	14.2 ± 0.6	3.8 ± 0.6	479 ± 19
	LSM		6.1 ± 0.2	29.4 ± 0.4		14.9 ± 0.9	2.7 ± 0.9	477 ± 25
	LSC		2.4 ± 0.3	26.3 ± 0.2		8.1 ± 0.8	3.3 ± 0.8	273 ± 17
	LSCM		1.6 ± 0.1	26.3 ± 0.4		7.3 ± 0.8	4.1 ± 0.8	270 ± 21
	LSI		5.2 ± 0.3	27.1 ± 0.2		11.7 ± 0.8	1.3 ± 0.8	337 ± 27
	QS		10.2 ± 0.3	37.3 ± 0.2		26.9 ± 0.8	6.5 ± 0.8	1071 ± 21
	SC		7.2 ± 0.1	27.9 ± 0.1		14.5 ± 0.5	0.1 ± 0.5	406 ± 5
	SCM		5.9 ± 0.1	22.0 ± 0.0		7.3 ± 0.4	−4.5 ± 0.4	94 ± 3

3.3. AF efficiency in the surfactant solutions studied

3.3.1. Effect of surfactant type on the AF activity at fixed surfactant concentration

First, we measured the foamability of the various surfactant solutions (without AF), applying a series of 50 shaking cycles, Fig. 7A. This number of cycles was chosen to ensure that the maximum foam volume, V_{50}, is reached for each surfactant solution in the absence of AF.

The comparison of the results shown in Fig. 7A reveals that the presence of MAc and Ca^{2+} in the LSM solution leads to significant reduction in the foam volume, certainly due to the formation of soap precipitates which can act as antifoam entities [38–40]. Foaming experiments with the SC and SCM solutions, in the absence of Ca^{2+}, showed no effect of MAc on the foamability, because no precipitates were formed in these solutions. All other formulations had also relatively high foamability, except for QS which adsorbs very slowly (cf. Fig. 3) and, hence, the foamability of this solution was relatively low, although the formed foam was very stable.

The addition of 3×10^{-4} wt. % AF in these solutions had significant impact on the foamability of LS, LSM, LSCM and LSI solutions, intermediate effect for LSC, and practically no effect for QS, SC and SCM solutions, Fig. 7A. To quantify the AF activity, we determined the ratio between the foam volumes formed in the presence and in the absence of AF after 50 shaking cycles – the ratio of these two foam volumes, measured with and without AF, can be used as a quantitative measure of the initial AF activity in the respective surfactant solution. The obtained results are shown in Fig. 7B, as a function of the area-per-molecule in the adsorption layer of the respective solution. One sees that the ratio of the foam volumes rapidly decreases with the increase of the area-per-molecule in the adsorption layer which indicates much higher antifoam activity in surfactant solutions with larger area-per-molecule. The antifoam is almost inactive, $V_{AF}/V_{50} \approx 1$, for SC and SCM solutions, both containing SLES + CAPB with relatively small mean area-per-molecule in the respective mixed adsorption layers.

We excluded the data for QS from the linear dependence shown in Fig. 7B, because the strong attraction between the saponin molecules within the respective adsorption layer leads to surface condensation, an extra-high surface dilatational elasticity, and related very low activity of the studied AF. Therefore, the systems with highly elastic adsorption layers do not obey the linear dependence shown in Fig. 7B.

Combining all experimental results discussed so far, we can conclude that: (1) The *in situ* formed MAc + Ca^{2+} soaps have significant antifoam effect even in the absence of PDMS-based AF. (2) The activity of the PDMS-silica AF in solutions of synthetic surfactants depends strongly on the ability of the surfactant molecules to form dense adsorption layer, with small mean area-per-molecule, on the bubble surface. The denser adsorption layers increase the stability of the pseudo-emulsion film, formed between the antifoam globules and the air-water interface, thus suppressing the entry of the AF globules on the solution surface. (3) The AF activity is very low also in QS solutions, because this saponin forms condensed adsorption layers with very high surface elasticity. This peculiar behaviour of the triterpenoid saponins is due to strong attraction between the adsorbed saponin molecules which leads to the formation of highly elastic, tightly packed adsorption layers, even at

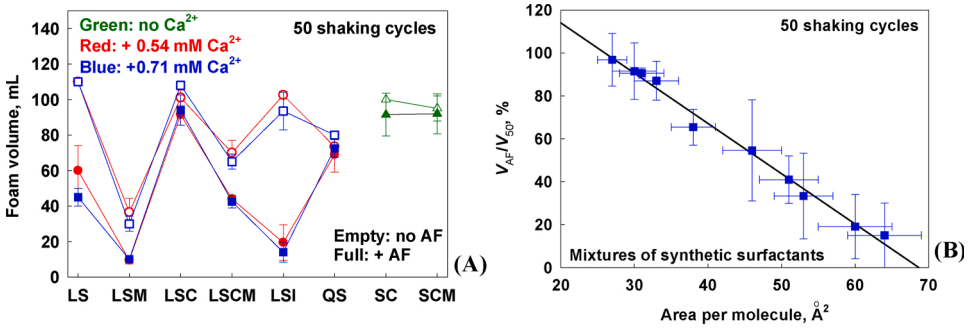

Fig. 7. (A) Foam volume for different surfactant solutions in the absence (empty symbols) and in the presence of AF (full symbols) after 50 shaking cycles in the Bartsch test. (B) Ratio between the foam formed in the presence of AF, V_{AF}, and in the absence of AF, V_{50}, after 50 shaking cycles, as a function of the area-per-molecule in the adsorption layers. The AF concentration is 3×10^{-4} wt. % and the experiments are performed at 40 °C.

relatively large area-per-molecule, see Fig. 2F and Ref. [47].

3.3.2. Effects of the surfactant and AF concentrations of the AF activity

To study the effects of surfactant concentration on the AF activity (at fixed AF concentration) and of AF concentration (at fixed surfactant concentration), we selected the solutions of LSI and LSC in 0.54 mM Ca^{2+} at pH ≈ 8.0, because these solutions are characterized with relatively large and relatively small area-per-molecule, respectively (cf. Table 1). The foam volumes in the presence of AF were measured after 10 shake cycles in the Barstch test and, then, compared to those measured after 10 cycles in the absence of AF.

The results for the effect of surfactant concentration at fixed AF concentration are shown in Fig. 8. One sees that the foam volume increases with the surfactant concentration for both studied solutions, with and without AF, as expected [30]. For the LSC solution, the ratio $V_{AF}/V_{10} \approx 80$ % for the two highest concentrations and ≈ 60 % for the lower concentrations. Such a trend is also expected, because the density of the adsorption layers is lower at the lower surfactant concentrations which facilitates the entry of the AF globules and enhances the overall AF activity. Note that the ratio V_{AF}/V_{10} varies in a relatively narrow range within the range of surfactant concentrations of interest, whereas both V_{AF} and V_{10} increase by > 5-fold with the increase of surfactant concentration. Therefore, due to this relatively weak dependence on the surfactant concentration, the ratio V_{AF}/V_{10} is a rather convenient measure of the AF activity for a given solution.

Similar experiments with LSI again showed less foam in the presence of antifoam: $V_{AF}/V_{10} \approx 25$ % for the three highest concentrations. It was difficult to determine precisely the ratio V_{AF}/V_{10} for the two lowest concentrations, because the value of V_{10} is very small and uncertain, which creates a relatively large error in the value of V_{AF}/V_{10}.

To quantify the effect of AF concentration, we performed another series of experiments in which this concentration was varied between 3×10^{-5} and 3×10^{-3} wt. %. Surfactant concentration was fixed at 0.17 wt. % and 0.54 mM Ca^{2+} solution was used to dilute the surfactant concentrates in this series. One sees from Fig. 9 that the foamability of LSI is strongly reduced, even at very low AF concentration of 3×10^{-5} wt. %, which shows that the AF is very active in this surfactant solution. Due to the large area-per-molecule in the adsorption layers formed on the bubble surface, the antifoam globules can enter easily the air-water interface and break the respective foam films.

In contrast, when the LSC formulation is used, the foamability is affected strongly only when the AF concentration increases up to ca. 3×10^{-3} wt. %. This more important impact of the AF concentration in the LSC solution is explained with the higher entry barrier which reduces the probability for AF globule entry. Therefore, higher concentration of AF globules is needed to ensure breakage of significant fraction of the foam films formed during foaming.

Note that the studied antifoam acts mostly during the foaming process when the foam films between the colliding bubbles are relatively thick. Therefore, the foam film rupture by the antifoam occurs in the process of foam film thinning when the Marangoni effects are controlling the rate of film thinning [30,31]. The antifoam entities rupture the thinning foam films via the so-called "bridging-stretching mechanism" as explained in Section 3.4.

From these series of experiments we conclude that the antifoam activity, expressed through the ratio V_{AF}/V_{10}, depends strongly on the antifoam concentration, while it is weakly affected by the surfactant concentration in the range of interest.

3.3.3. Role of surfactant composition and surface properties for the AF durability

The AF durability characterises for how long the AF can destroy newly generated foam under given conditions. To quantify the foam evolution in the studied solutions, we fitted the experimental data for the foam volume vs. the number of shaking cycle by the empirical equation [30]:

$$V(n) = V_\infty(1 - \exp(-n/n_0)) \quad (6)$$

Here V_∞ is the maximum volume of air which would be entrapped after a very large number of cycles, n is the number of the respective cycle at which $V(n)$ is measured, and n_0 is the characteristic number of cycles at which V reaches ≈ 63 % of V_∞. We found that this equation describes very well the data both in the absence and in the presence of AF. As expected, typically the value of V_∞ in the presence of AF is lower while n_0 is larger, reflecting the fact that the AF decreases both the final foam volume and the rate of foam generation.

In Fig. 10A we show the results for the ratio $V_{AF\infty}/V_\infty$ determined in the presence and in the absence of AF for the different solutions. One sees that the studied AF is very active even after 1000 shaking cycles in LSI solution and has some activity in the solutions of the other surfactants with low Ca^{2+} concentration, whereas almost the same foam volumes are measured with and without AF after 1000 shaking cycles for the solutions with higher Ca^{2+} concentration.

To quantify the AF durability, we compared the values of n_0 in the presence and in the absence of AF, however, this time defined as the number of cycles which are required to reach 63 % of the final foam without AF, viz. V_∞. The ratio of these two values, shown in Fig. 10B, gives information on how many times we should increase n_0 in the presence of AF to reach 63 % of V_∞. One sees that this ratio is relatively small for LSC, QS, SC and SCM solutions, i.e. the AF durability is rather low in these four solutions at 3×10^{-4} wt. % AF (longer durability is expected at higher AF concentrations). Intermediate durability is determined in LS, LSM and LSCM solutions in which ≈ 5-fold increase of the shaking cycles is needed to reach 63 % of V_∞. More than 50-fold increase of the shaking cycles is required for LSI, thus illustrating the very high durability of the AF in this solution.

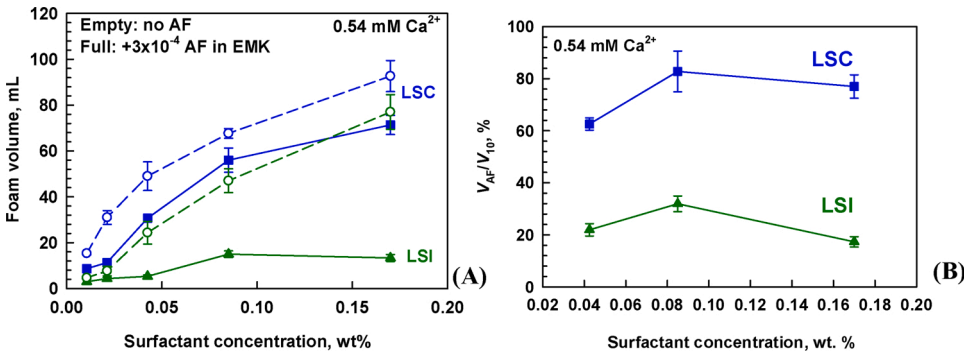

Fig. 8. (A) Foam volume as a function of surfactant concentration in the absence (empty symbols) and in the presence of 3×10^{-4} wt. % AF pre-dispersed in EMK (full symbols), at fixed surfactant concentration of 0.17 wt. % in the presence of 0.54 mM Ca^{2+}. (B) Same data plotted as a ratio of the foam volumes with and without antifoam, V_{AF}/V_{10}. Data are obtained after 10 shaking cycles in the Bartsch test at 40 °C.

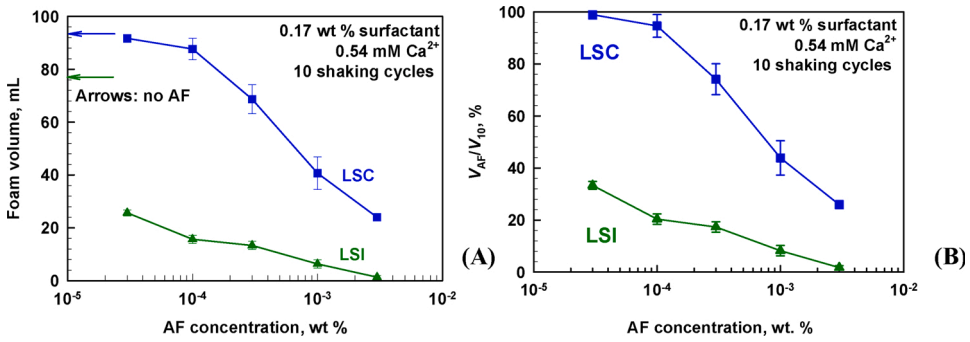

Fig. 9. (A) Foam volume, V_{AF}, versus antifoam concentration at fixed surfactant concentration of 0.17 wt. %, in the presence of 0.54 mM Ca^{2+}. The arrows show the foam volume, V_{10}, of the same solutions in the absence of AF. (B) Same data plotted as V_{AF}/V_{10}. Foam volumes are measured after 10 shaking cycles in the Bartsch test at 40 °C.

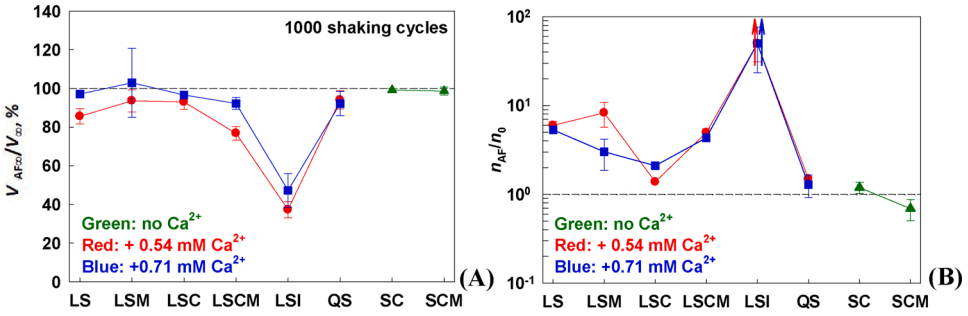

Fig. 10. (A) Ratio between the foam volume which is generated after 1000 shake cycles in the presence of 3×10^{-4} wt. % AF (predispersed in EMK) and the maximum foam volume generated by the same surfactant solutions without AF, V_∞. (B) Ratio of the number of shake cycles, with and without AF, required to reach 63 % of the maximum foam volume, V_∞. The arrows for the LSI system in (B) indicate that the increase in the number of shaking cycles for this mixture was > 50-fold; the exact values were not determined for this system, because of the very long duration of the respective experiment.

We conclude that the surfactant type significantly affects the AF durability under otherwise equivalent conditions. In the solutions with dense adsorption layer and/or with high surface dilatational modulus, both the AF activity and durability are much lower when compared to those in solutions with loose adsorption layers and low surface modulus.

3.4. Mechanism of AF action in the studied surfactant solutions

To determine which mechanism is operative in the studied systems, we performed microscope observations of foam films in the presence of AF globules. In these experiments we observed the formation of a characteristic circular pattern in the foam films (series of bright and dark concentric fringes of diameter ca. 10 μm), just before the foam film rupture – see Fig. 11 for illustrative image. This pattern, called "fish-eye" due to its specific appearance [8], was identified in the literature to reflect the formation of an oil bridge between the two foam film surfaces which rapidly expands in radial direction, due to uncompensated capillary pressures at the various interfaces, thus leading to a bridging-stretching mechanism of foam film rupture [8]. The illustrative image in Fig. 11 presents such an oil bridge in foam film formed from LSI solution and similar observations were made with LS and LSC solutions. Fig. 11B compares the characteristic life-times of the formed oil bridges which turned out to be very short – the foam films ruptured within 20–100 ms after the formation of the first oil bridge in their interior.

Thus, we conclude that the bridging-stretching mechanism was responsible for the foam film rupture in the systems studied.

4. Summary and conclusions

The main results from this study could be summarized as follows:

1 The most important and interesting result is the observed strong correlation between the initial antifoam activity and the mean area-per-molecule in the mixed surfactant adsorption layers, formed at the

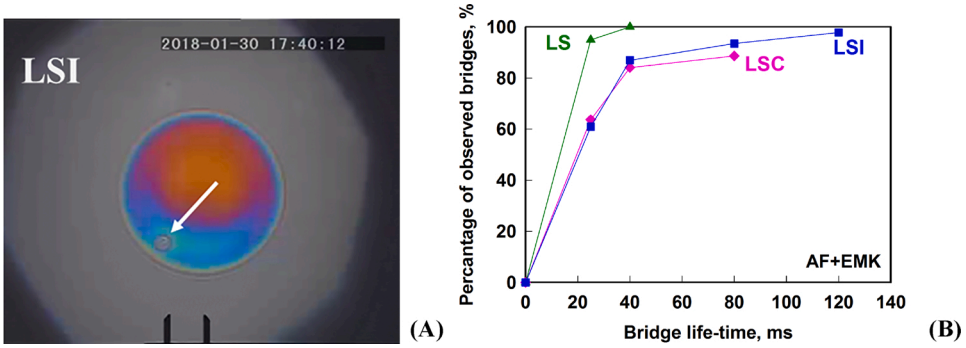

Fig. 11. (A) Image of a foam film with an oil bridge, shown by arrow, just before the foam film rupture; this foam film is formed from 0.17 wt. % solution of LSI mixture. (B) Probability for rupture of the oil bridges, as a function of the bridge lifetime. The AF concentration in these experiments is 3×10^{-3} wt. %, i.e. higher than in the main foaming experiments, to increase the probability for observation of film rupture in the capillary cell.

air-water interface. The antifoam is much more active in solutions which form adsorption layers with larger area-per-molecule for all studied synthetic surfactants with low molecular mass. With this trend we could explain the opposite effects of surfactants which lead to denser adsorption layers and reduce the antifoam activity (e.g. the zwitterionic CAPB) versus the nonionic surfactants with large headgroup which enhance the antifoam action (e.g. alkylethoxylated nonionic surfactants) under otherwise equivalent conditions.

2 Several other effects related to the AF activity deserve to be emphasized:

3) The presence of myristic acid and Ca^{2+} ions in the solution can lead to precipitated calcium soaps which also have antifoam effect, even in the absence of silicone-based antifoams.

4) The presence of myristic acid at room temperature and pH $\approx$ 6, without Ca^{2+} in the solution, leads to formation of condensed adsorption layer which blocks the spreading of the PDMS-based antifoam on the surface and, also, strongly decreases the antifoam activity and durability.

5) The natural surfactant QS (triterpenoid saponin) adsorbs relatively slowly on the bubble surface but forms highly elastic condensed adsorption layers which hinder the spreading of PDMS even at highly positive spreading coefficient, $S \approx 6.5$ mN/m, and suppress the antifoam activity of the PDMS-silica compound.

6 The exhaustion of the AF is much faster in the solutions with denser adsorption layers, due to the higher entry barriers in these systems.

7 Although the effect of surfactant concentration on the antifoam activity is rather strong, the relative decrease of the foam volume caused by the antifoam is a weak function of the surfactant concentration (though it varies strongly with the surfactant composition). On the other hand, as expected, the increase of the antifoam concentration significantly increases the antifoam activity and durability, under otherwise equivalent conditions.

All these results and conclusions provide self-consistent explanations of the observed experimental trends and suggest approaches for rational design of surfactant mixtures with desired foam control in the presence of PDMS-based antifoams.

CRediT authorship contribution statement

N. Politova-Brinkova: Methodology, Formal analysis, Visualization, Writing - original draft. **M. Hristova:** Investigation, Validation. **V. Georgiev:** Investigation, Validation. **S. Tcholakova:** Conceptualization, Methodology, Formal analysis, Writing - review & editing, Supervision, Funding acquisition. **N. Denkov:** Conceptualization, Writing - review & editing, Funding acquisition. **M. Grandl:** Conceptualization, Funding acquisition. **F. Achenbach:** Conceptualization, Funding acquisition.

Declaration of Competing Interest

The authors report no declarations of interest.

Acknowledgements

M. Hristova acknowledges the financial support from the program “Young scientists and Postdoctoral candidates" of the Bulgarian Ministry of Education and Science, MCD No 577/17.08.2018. This work was supported by Wacker Chemie AG, Germany. The authors are grateful to Mrs. Dora Dimitrova for performing the interfacial tension measurements.

Appendix A. Supplementary data

Supplementary material related to this article can be found, in the online version, at doi:https://doi.org/10.1016/j.colsurfa.2020.125747.

References

[1] P.R. Garrett, The science of defoaming theory. Experiment and Applications, CRC Press, Boca Raton, 2014.
[2] R.J. Pugh, Foaming, foam films, antifoaming and defoaming, Adv. Colloid Interface Sci. 64 (1996) 67–142, https://doi.org/10.1016/0001-8686(95)00280-4.
[3] N.D. Denkov, K.G. Marinova, Antifoam effects of solid particles, oil drops and oil–solid compounds in aqueous foams, in: B.P. Binks, T.S. Horozov (Eds.), Colloidal Particles at Liquid Interfaces., Cambridge University Press, 2006, pp. 383–444.
[4] N.D. Denkov, Mechanisms of foam destruction by oil-based antifoams, Langmuir 20 (2004) 9463–9505, https://doi.org/10.1021/la049676o.
[5] A. Dippenaar, The destabilization of froth by solids. I. The mechanism of film rupture, Int. J. Miner. Process. 9 (1982) 1–14, https://doi.org/10.1016/0301-7516(82)90002-3.
[6] R. Aveyard, P. Cooper, P.D. Fletcher, C.E. Rutherford, Foam breakdown by hydrophobic particles and nonpolar oil, Langmuir 9 (1993) 604–613, https://doi.org/10.1021/la00026a041.
[7] G.C. Frye, J.C. Berg, Mechanisms for the synergistic antifoam action by hydrophobic solid particles in insoluble liquids, J. Colloid Interface Sci. 130 (1989) 54–59, https://doi.org/10.1016/0021-9797(89)90077-5.
[8] N.D. Denkov, P. Cooper, J.-Y. Martin, Mechanisms of action of mixed solid–liquid antifoams. 1. Dynamics of foam film rupture, Langmuir 15 (1999) 8514–8529, https://doi.org/10.1021/la9902136.
[9] E.S. Basheva, D. Ganchev, N.D. Denkov, K. Kasuga, N. Satoh, K. Tsujii, Role of betaine as foam booster in the presence of silicone oil drops, Langmuir 16 (2000) 1000–1013, https://doi.org/10.1021/la990777.
[10] A. Hadjiiski, S. Tcholakova, N.D. Denkov, P. Durbut, G. Broze, A. Mehreteab, Effect of oily additives on the foamability and foam stability. 2. Entry barriers, Langmuir 17 (2001) 7011–7021, https://doi.org/10.1021/la010601j.
[11] N.D. Denkov, S. Tcholakova, K.G. Marinova, A. Hadjiiski, Role of oil spreading for the efficiency of mixed oil–solid antifoams, Langmuir 18 (2002) 5810–5817, https://doi.org/10.1021/la020073r.
[12] A. Hadjiiski, N.D. Denkov, S. Tcholakova, I.B. Ivanov, Role of entry barriers in the foam destruction by oil drops, in: K. Mittal, D. Shah (Eds.), Adsorption and Aggregation of Surfactants in Solution, Marcel Dekker, 2002, pp. 465–500. Chapter 23.
[13] A. Hadjiiski, S. Tcholakova, I.B. Ivanov, T.D. Gurkov, E.F. Leonard, Gentle film trapping technique with application to drop entry measurements, Langmuir 18 (2002) 127–138, https://doi.org/10.1021/la010751u.
[14] N.D. Denkov, K.G. Marinova, S.S. Tcholakova, Mechanistic understanding of the modes of action of foam control agents, Adv. Colloid Interface Sci. 206 (2014) 57–67, https://doi.org/10.1016/j.cis.2013.08.004.
[15] Thin liquid films: fundamentals and applications, in: P.M. Kruglyakov, I.B. Ivanov (Eds.), Surfactant Science Series, Marcel Dekker, New York, 1988, https://doi.org/10.1002/aic.690350825. Chapter 11.
[16] R.D. Kulkarni, E.D. Goddard, B. Kanner, Mechanism of antifoaming action, J. Colloid Interface Sci. 59 (1977) 468–476, https://doi.org/10.1016/0021-9797(77)90042-X.
[17] P.R. Garrett, J. Davis, H.M. Rendall, An experimental study of the antifoam behaviour of mixtures of a hydrocarbon oil and hydrophobic particles, Colloids Surf. A. Physicochem. Eng. Aspects 85 (1994) 159–197, https://doi.org/10.1016/0927-7757(93)02678-8.
[18] K.G. Marinova, N.D. Denkov, Foam destruction by mixed solid–liquid antifoams in solutions of alkyl glucoside: electrostatic interactions and dynamic effects, Langmuir 17 (2001) 2426–2436, https://doi.org/10.1021/la001558n.
[19] E.S. Basheva, S. Stoyanov, N.D. Denkov, K. Kasuga, N. Satoh, K. Tsujii, Foam Boosting by Amphiphilic Molecules in the Presence of Silicone Oil, Langmuir 17 (2001) 969–979, https://doi.org/10.1021/la001106a.
[20] P.R. Garrett, P.R. Garrett (Eds.), Defoaming: Theory and Industrial Applications, Marcel Dekker, New York, 1993, https://doi.org/10.1002/jctb.280590130.
[21] N.D. Denkov, K.G. Marinova, C. Christova, A. Hadjiiski, Ph. Cooper, Mechanisms of action of mixed solid-liquid antifoams: 3. Exhaustion and reactivation, Langmuir 16 (2000) 2515–2528, https://doi.org/10.1021/la9910632.
[22] N.D. Denkov, Mechanisms of action of mixed solid-liquid antifoams. 2. Stability of oil bridges in foam films, Langmuir 15 (1999) 8530–8542, https://doi.org/10.1021/la990214y.
[23] A. Passerone, L. Liggieri, M. Rando, F. Ravera, E. Ricci, A new experimental method for measurement of the interfacial tension between immiscible fluids at zero bond number, J. Colloid Interface Sci. 146 (1991) 152–162, https://doi.org/10.1016/0021-9797(91)90012-W.
[24] D. Möbius, R. Miller (Eds.), Drops and Bubbles in Interfacial Research, Elsevier, Amsterdam, 1998.
[25] S.C. Russev, N.A. Alexandrov, K.G. Marinova, K.D. Danov, N.D. Denkov, L. Lyutov, V. Vulchev, C. Bilke-Krause, Instrument and methods for surface dilatational rheology measurements, Rev. Sci. Instrum. 79 (2008) 104102, https://doi.org/10.1063/1.3000569.
[26] N.A. Alexandrov, K.G. Marinova, K.D. Danov, I.B. Ivanov, Surface dilatational rheology measurements for oil/water systems with viscous oils, J. Colloid Interface Sci. 339 (2009) 545–550, https://doi.org/10.1016/j.jcis.2009.08.002.
[27] Y. Rotenberg, L. Boruvka, A.W. Neumann, Determination of surface tension and contact angle from the shapes of axisymmetric fluid interfaces, J. Colloid Interface Sci. 93 (1983) 169–183, https://doi.org/10.1016/0021-9797(83)90396-X.
[28] A. Scheludko, Thin liquid films, Adv. Colloid Interface Sci. 1 (1967) 391–464, https://doi.org/10.1016/0001-8686(67)85001-2.

[29] P.A. Kralchevsky, K. Nagayama, Particles at Fluid Interfaces and Membranes, Elsevier, Amsterdam, 2001. Chapter 14.
[30] B. Petkova, S. Tcholakova, M. Chenkova, K. Golemanov, N. Denkov, D. Thorley, S. Stoyanov, Foamability of aqueous solutions: Role of surfactant type and concentration, Adv. Colloid Interface Sci. 276 (2020) 102084, https://doi.org/10.1016/j.cis.2019.102084.
[31] P.A. Kralchevsky, K.D. Danov, N.D. Denkov, Chemical physics of colloid systems and interfaces., editor. Chapter7 in, in: K.S. Birdi (Ed.), Handbook of Surface and Colloid Chemistry, 3rd updated ed., CRC Press, Boca Raton, FL, 2008.
[32] S.E. Anachkov, S. Tcholakova, D.T. Dimitrova, N.D. Denkov, N. Subrahmaniam, P. Bhunia, Adsorption of linear alkyl benzene sulfonates on oil–water interface: Effects of Na^{+}, Mg^{2+} and Ca^{2+} ions, Colloids Surf. A Physicochem. Eng. Asp. 446 (2015) 18–27, https://doi.org/10.1016/j.colsurfa.2014.10.059.
[33] F. Mustan, A. Ivanova, S. Tcholakova, N. Denkov, Revealing the origin of the specificity of calcium and sodium cations binding to adsorption monolayers of two anionic surfactants, J. Phys. Chem. B., under review.
[34] K.D. Danov, S.D. Kralchevska, P.A. Kralchevsky, K.P. Ananthapadmanabhan, A. Lips, Mixed Solutions of Anionic and Zwitterionic Surfactant (Betaine): Surface Tension Isotherms, Adsorption and Relaxation Kinetics, Langmuir 20 (2004) 5445–5453, https://doi.org/10.1021/la049576i.
[35] Z. Mitrinova, S. Tcholakova, K. Golemanov, N. Denkov, M. Vethamuthu, K. P. Ananthapadmanabhan, Surface and foam properties of SLES + CAPB + fatty acid mixtures: effect of pH for C12–C16 acids, Colloids and Surfaces A: Physicochem. Eng. Aspects 438 (2013) 186–198, https://doi.org/10.1016/j.colsurfa.2012.12.011.
[36] Z. Mitrinova, S. Tcholakova, Z. Popova, N. Denkov, B.R. Dasgupta, K. P. Ananthapadmanabhan, Efficient Control of the Rheological and Surface Properties of Surfactant Solutions Containing C8−C18 Fatty Acids as Cosurfactants, Langmuir 29 (2013) 8255–8265, https://doi.org/10.1021/la401291a.
[37] R. Stanimirova, K. Marinova, S. Tcholakova, N.D. Denkov, S. Stoyanov, E. Pelan, Surface Rheology of Saponin Adsorption Layers, Langmuir 27 (2011) 12486–12498, https://doi.org/10.1021/la202860u.
[38] H. Zhang, C.A. Miller, P.R. Garrett, K.H. Raney, Mechanism for defoaming by oils and calcium soap in aqueous systems, J. Colloid Interface Sci. 263 (2003) 633–644, https://doi.org/10.1016/S0021-9797(03)00367-9.
[39] H. Zhang, C.A. Miller, P.R. Garrett, K.H. Raney, Defoaming effect of calcium soap, J. Colloid Interface Sci. 279 (2004) 539–547, https://doi.org/10.1016/j.jcis.2004.06.103.
[40] H. Zhang, C.A. Miller, P.R. Garrett, K.H. Raney, Lauryl alcohol and amine oxide as foam stabilizers in the presence of hardness and oily soil, J. Surfactants Deterg. 8 (2005) 99–107, https://doi.org/10.1007/s11743-005-0337-3.
[41] R. Aveyard, J.H. Clint, Liquid droplets and solid particles at surfactant solution interfaces, J Chem Soc Faraday Trans. 91 (1995) 2681–2697, https://doi.org/10.1039/FT9959102681.
[42] R. Aveyard, B.P. Binks, P.D.I. Fletcher, T.-G. Peck, P.R. Garrett, Entry and spreading of alkane drops at the air/surfactant solution interface in relation to foam and soap film stability, J. Chem. Soc. Faraday. Trans. 89 (1993) 4313–4321, https://doi.org/10.1039/FT9938904313.
[43] R. Aveyard, B.P. Binks, P.D.I. Fletcher, T.-G. Peck, C.E. Rutherford, Aspects of aqueous foam stability in the presence of hydrocarbon oils and solid particles, Adv. Colloid Interface Sci. 48 (1994) 93–120, https://doi.org/10.1016/0001-8686(94)80005-7.
[44] R. Aveyard, B.D. Beake, J.H. Clint, Wettability of spherical particles at liquid surfaces, J. Chem. Soc. Faraday Trans. 92 (1996) 4271–4277, https://doi.org/10.1039/FT9969204271.
[45] P.R. Garrett, Preliminary considerations concerning the stability of a liquid heterogeneity in a plane-parallel liquid film, J. Colloid Interface Sci. 76 (1980) 587–590, https://doi.org/10.1016/0021-9797(80)90400-2.
[46] Q.S. Bhatia, J.-K. Chen, J.T. Koberstein, J.E. Sohn, J.A. Emerson, The measurement of polymer surface tension by drop image processing: application to PDMS and comparison with theory, J. Colloid Interface Sci. 106 (1985) 353–359, https://doi.org/10.1016/S0021-9797(85)80009-6.
[47] N. Pagureva, S. Tcholakova, K. Golemanov, N. Denkov, E. Pelan, S.D. Stoyanov, Surface properties of adsorption layers formed from triterpenoid and steroid saponins, Colloids and Surfaces A: Physicochem, Eng. Aspects 491 (2016) 18–28, https://doi.org/10.1016/j.colsurfa.2015.12.001.